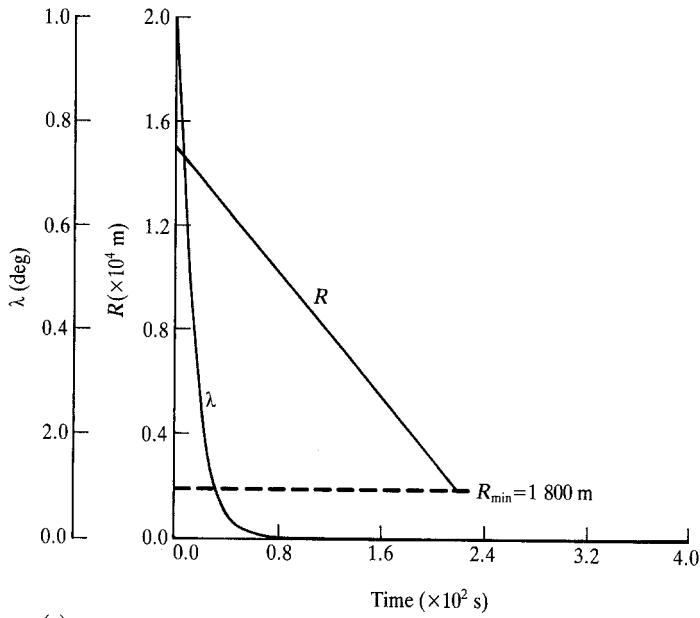


Figure 11.36 Location of ILS ground transmitters and antennas.

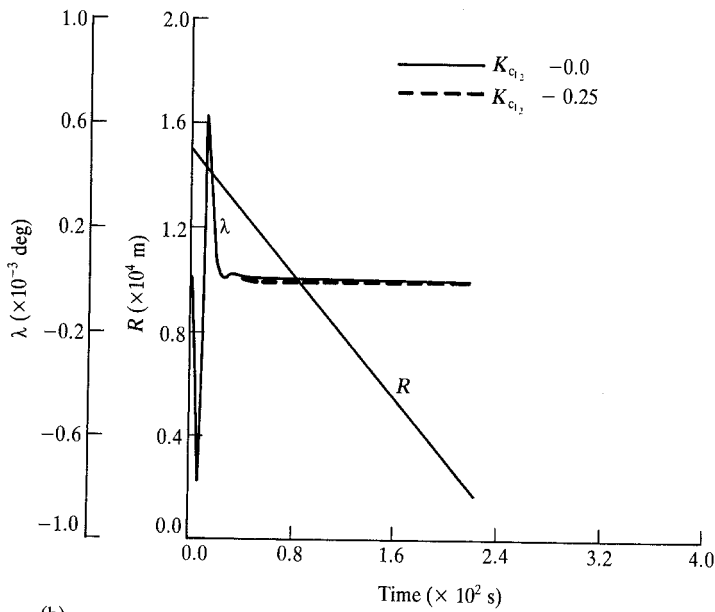
except that Γ represents the angular deviation from the localizer centre-line, and a localizer receiver is used, not the VOR receiver denoted. More care must be exercised with the controller gains since the beamwidth of the system is less ($\sim 3^\circ$). There are also present in the transfer function representing the localizer receiver, the dynamics associated with the low-pass filters needed to remove the 90 and 150 Hz modulation tones from the output signals. The range involved in this system is much less than that which obtains with VOR coupling, being not greater than about fifteen miles, usually less. However, like the VOR hold system, the localizer-coupled control system cannot operate below a certain minimum value of range, otherwise the open loop gain will increase beyond the critical value and the closed loop system will become unstable. The response of a digital simulation of an ILS localizer-coupled control system to an initial angular displacement of 1° to the right, at a range of 15 000 m, for CHARLIE-1, is shown in Figure 11.37(a). The corresponding values of gains are shown in Table 11.2. The minimum value of range for stability is approximately 200 m; the simulation was stopped when the range reached 1 800 m. This simulation was only illustrative since the airspeed was maintained at a constant value of $U_0 = 60.0 \text{ m s}^{-1}$. The response of the same system to a crosswind corresponding to a side gust of $\pm 1^\circ$ in 10 s, and with the airspeed being reduced steadily from 60 to 40 m s^{-1} throughout the approach, is shown in Figure 11.37(b). Note how effectively the system restores the aircraft to the localizer centre-line and maintains it there: the peak displacement in heading is only 8×10^{-4} degrees. The dotted line represents the trajectory corresponding to $K_{c12} = 0.25 \text{ s}^{-1}$. In Figure 11.37(c) the trajectory is shown for an initial range of 40 000 m and a constant speed of 158 m s^{-1} ; the purpose of including this trajectory is to show the behaviour of the system when minimum range is approached and reached: the system becomes unstable.

11.9 ILS GLIDE-PATH-COUPLED CONTROL SYSTEM

This system uses the output signal from the airborne glide path receiver as a guidance command to the attitude control system of the aircraft. The loop is

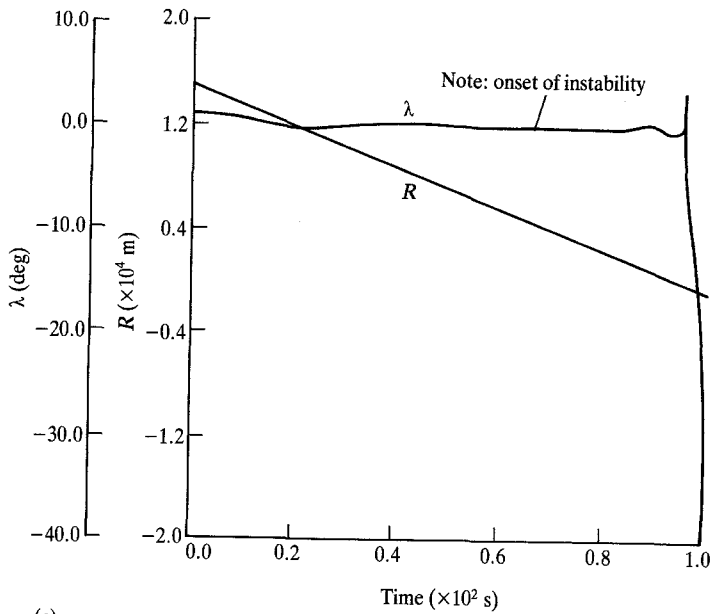


(a)



(b)

Figure 11.37 (a) ILS-coupled trajectory. (b) Response to side gust.



(c)

(c) Unstable response.

Table 11.2 Gains for ILS localizer-coupled system

$K_\lambda = 1.0$	$K_c = 15.0$	$K_{c_{12}} = 0.0$
$U_0 = 60 \text{ m s}^{-1}$	$R_0 = 15 \times 10^3 \text{ m}$	

closed via the aircraft kinematics which transform the pitch attitude of the aircraft into a displacement from the preferred descent path (the glide path) into the airport. The situation is represented in Figure 11.38(a). The glide path angle is denoted by γ_G and its nominal value is -2.5° . If an aircraft is flying into an airport, but it is displaced below the glide path by a distance, d , that distance is negative. The geometry is shown in Figure 11.38(b). If the value of the aircraft's own flight path angle is -2.5° , the displacement is 0. Any angular deviation from the centre-line of the glide path transmission is measured by the airborne glide path receiver: that deviation depends upon both the displacement, d , and the slant range from the transmitter. Since the value of γ_G is so small, it is customary to regard the slant and horizontal ranges, R and x , respectively, as identical; the correct relationship is, of course:

$$x = R \cos 2.5^\circ \quad (11.39)$$

In this section, x and R are taken as identical. Therefore, the angular deviation, Γ , is defined as:

$$\Gamma = d/R \quad (11.40)$$

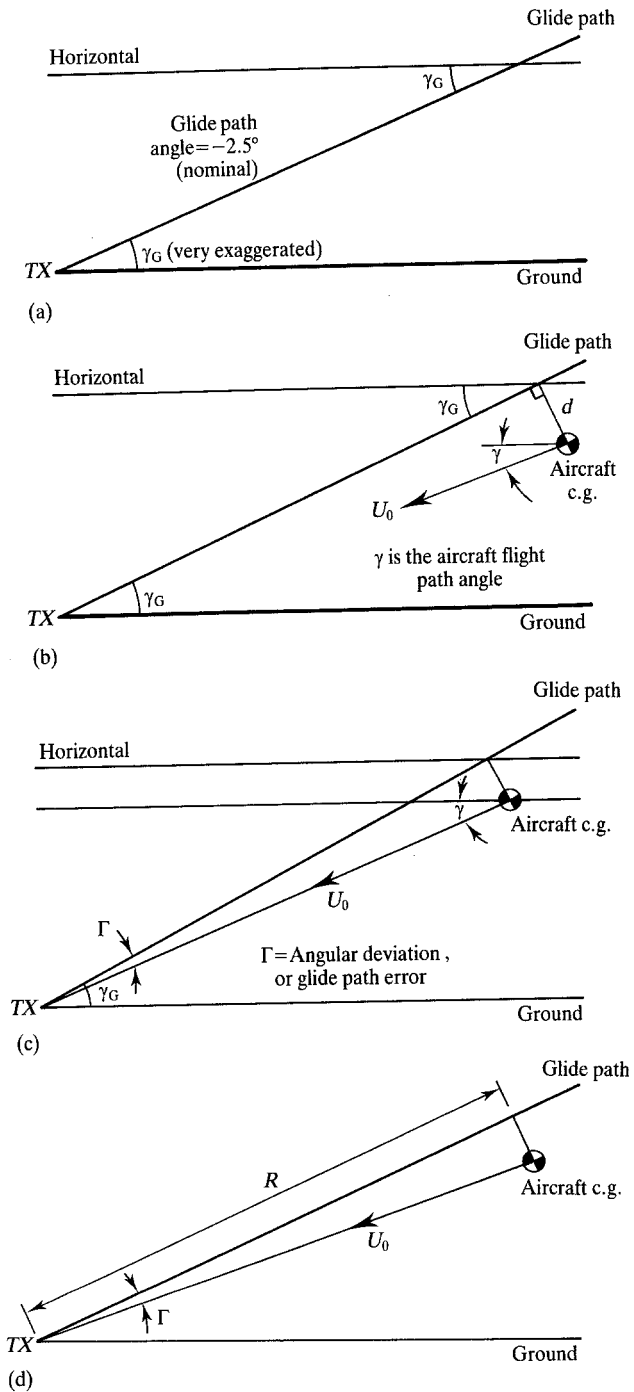


Figure 11.38 (a) The glide path geometry.
 (b) Aircraft below glide path – geometry.
 (c) Angular deviation from glide path – geometry.
 (d) Slant range definition.

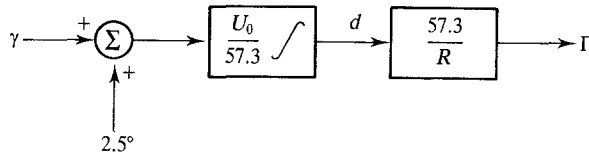


Figure 11.39 Block diagram of glide path measurement.

where Γ is in radians.

The component of the airspeed which is perpendicular to the glide path is $U_0 \sin \Gamma$; this quantity represents the rate of change of the displacement, i.e.:

$$\dot{d} = U_0 \sin \Gamma \approx (U_0/57.3)\Gamma \tag{11.41}$$

However, for the situation shown in Figure 11.38 the aircraft's flight path angle is less than 2.5° , therefore Γ is positive (note that $\Gamma = \gamma + 2.5^\circ$) and \dot{d} is positive. As the initial displacement was negative, and its rate of change is positive, the situation shown in Figure 11.38(c) represents the case when the aircraft is approaching the glide path from below:

$$d = (U_0/57.3) \int (\gamma + 2.5^\circ) dt = (U_0/57.3) \int \Gamma dt \tag{11.42}$$

The block diagram representing eq. (11.42) is shown in Figure 11.39.

The aircraft flight path angle, γ , is defined by:

$$\gamma = (\theta - \alpha) \tag{11.43}$$

Consequently, the flight path angle is most effectively controlled by using a pitch attitude control system, with a pitch rate SAS as an inner loop, to effectively

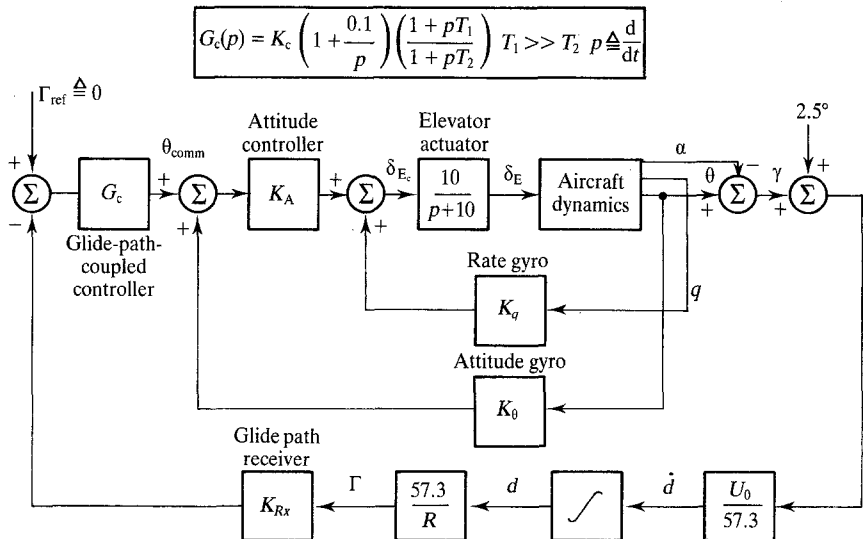


Figure 11.40 Glide-path-coupled control system.

control any changes in the angle of attack which may arise as a result of the elevator's being used to drive the aircraft back onto the glide path. The block diagram of a typical glide path control system is shown in Figure 11.40. The gain of the glide path receiver, K_{R_x} , can be considered, without loss of generality, to be 1 V deg^{-1} . The control law used is then:

$$\theta_{\text{comm}} = - G_c(p)\Gamma \tag{11.44}$$

The transfer function, G_c , of the glide-path-coupled controller represents essentially a proportional plus integral term controller. The phase advance term has been added to provide extra stabilization, if required. So far it has been presumed that the airspeed, U_0 , is constant throughout the coupled trajectory, but this is never the case. A speed control system, used in conjunction with the glide-path-coupled system, is essential to ensure that the aircraft's flight path angle, γ , in the steady state, has the same sign as the commanded pitch angle. The speed control system also ensures that the airspeed of the aircraft is reduced from U_{01} at the start of the approach to a lower value, U_{02} , at its finish, the change in speed corresponding to the appropriate speed schedule, $U_{\text{ref}}(t)$. A typical speed schedule, for CHARLIE-1, is given in Figure 11.41. At the start of the coupled glide path descent, the airspeed, U_{01} , is 85.0 m s^{-1} ; thirty seconds later, it is 65.0 m s^{-1} . During that time the aircraft will have travelled a slant distance of:

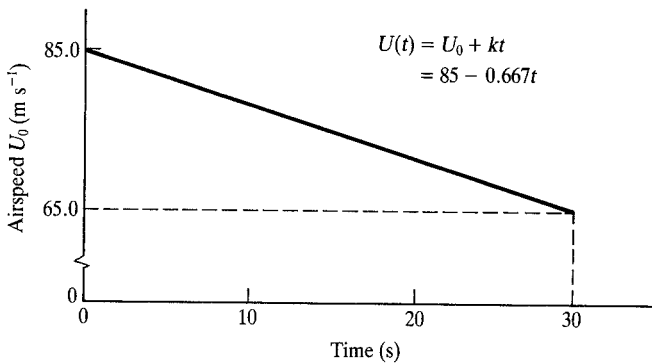


Figure 11.41 Airspeed schedule for CHARLIE-1.

$$R = \int_0^{30} (85 - 0.667t)dt = 2250 \text{ m} \tag{11.45}$$

The horizontal distance covered is actually 2248 m (assuming aircraft descends along the glide path). The height at the start of this manoeuvre is 320 ft. A typical set of parameters, corresponding to CHARLIE-1, is given in Table 11.3 and the corresponding dynamic response to an initial displacement, d , of 100 ft above the glide path, is shown in Figure 11.42. It is evident how effective the system is in restoring the aircraft to the glide path and maintaining it there subsequently.

Table 11.3 Parameters of glide-path-coupled system

$K_\theta = 1.0$	$K_A = 3.1$	$T_1 = 0.4$
$K_q = 1.9$	$K_c = -20.00$	$T_2 = 0.04$

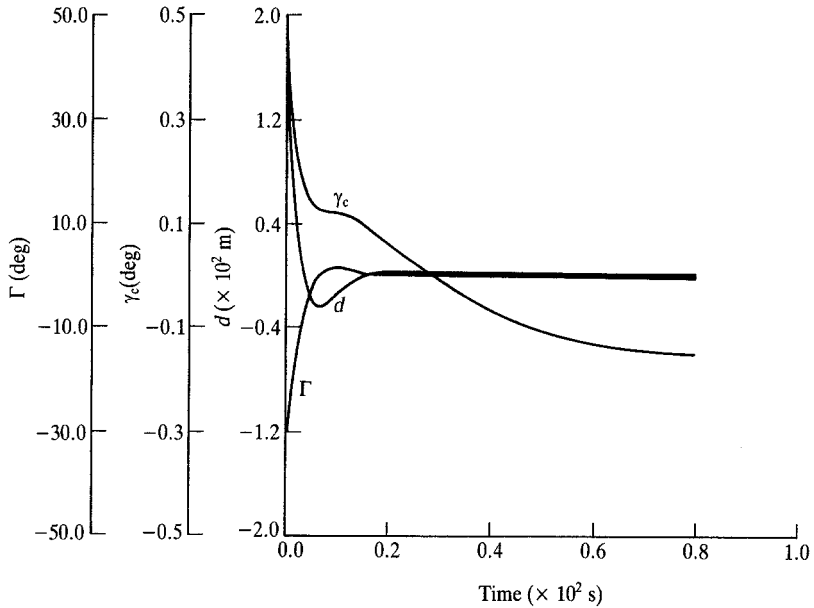


Figure 11.42 Response of glide-slope-coupled system.

For the system represented in Figure 11.40, and using the values of parameters listed in Table 11.3,³ it can be shown that the closed loop dynamics can be represented in that form, representing a generalized AFCS, which was explained in Section 7.2 of Chapter 7.

Aircraft dynamics

$$\dot{\mathbf{x}} = A\mathbf{x} + B\mathbf{u} \quad (11.46)$$

where:

$$\mathbf{x}' \triangleq [u \ w \ q \ \theta \ \delta_E] \quad (11.47)$$

$$\mathbf{u} \triangleq [\delta_{E_c}] \quad (11.48)$$

$$A = \begin{bmatrix} -0.021 & 0.122 & 0 & -9.81 & 0.292 \\ -0.2 & -0.512 & 65.1 & 0 & -1.96 \\ 0.00004 & -0.006 & -0.402 & 0 & -0.4 \\ 0 & 0 & 1 & 0 & 0 \\ 0 & 0 & 0 & 0 & -10 \end{bmatrix} \text{ for CHARLIE-1} \quad (11.49)$$

$$B' = [0 \ 0 \ 0 \ 0 \ 10] \tag{11.50}$$

Output equation

$$y = Cx \tag{11.51}$$

where:

$$y \triangleq [\alpha \ q \ \theta] \tag{11.52}$$

$$C = \begin{bmatrix} 0 & 0.015 & 0 & 0 & 0 \\ 0 & 0 & 1 & 0 & 0 \\ 0 & 0 & 0 & 1 & 0 \end{bmatrix} \tag{11.53}$$

Controller dynamics

$$\dot{x}_c = A_c x_c + B_c y + E \tag{11.54}$$

Controller output equation is:

$$y_c = C_c x_c + D_c y \tag{11.55}$$

with:

$$\delta_{E_c} \triangleq y_c \tag{11.56}$$

From Figure 11.40 and Table 11.3 it can be deduced that for the glide path coupled control system the control law is:

$$\begin{aligned} \delta_{E_c} &= K_q q + K_\theta K_A \theta - K_A K_c \frac{(1 + pT_1)}{(1 + pT_2)} \left\{ 1 + \frac{0.1}{p} \right\} \Gamma \\ &= 1.9q + 3.1\theta + 62.0 \frac{(1 + p0.4)}{(1 + p0.04)} \left\{ 1 + \frac{0.1}{p} \right\} \Gamma \end{aligned} \tag{11.57}$$

Furthermore, it can be seen that:

$$\begin{aligned} \Gamma &= \frac{U_0}{R} \int \theta dt - \frac{1}{R} \int w dt + 2.5 \frac{U_0}{R} t \\ &= \frac{65.1}{R} \int \theta dt - \frac{1}{R} \int w dt + \frac{162.75}{R} t \end{aligned} \tag{11.58}$$

If we let:

$$\int \theta dt \triangleq x_{c_1} \tag{11.59}$$

$$\int w dt \triangleq x_{c_2} \tag{11.60}$$

$$t \triangleq x_{c_3} \quad (11.61)$$

then

$$\Gamma = \frac{65.1}{R} x_{c_1} - \frac{1}{R} x_{c_2} + \frac{162.75}{R} x_{c_3} \quad (11.62)$$

If the third term on the r.h.s. of eq. (11.57) is denoted by $-K_A K_c g(p)$ then:

$$\begin{aligned} \frac{g(p)}{\Gamma(p)} &= \frac{p^2 T_1 + (1 + 0.1 T_1)p + 0.1}{p^2 T_2 + p} \\ &= \frac{0.4p^2 + 1.04p + 0.1}{0.04p^2 + p} \end{aligned} \quad (11.63)$$

Let:

$$\frac{g(p)}{\Gamma(p)} = \frac{g(p)}{z(p)} \cdot \frac{z(p)}{\Gamma(p)} = (0.4p^2 + 1.04p + 0.1) \frac{1}{0.04p^2 + p} \quad (11.64)$$

Then:

$$0.04\ddot{z} + z = \Gamma \quad (11.65)$$

$$0.4\ddot{z} + 1.04\dot{z} + 0.1z = g \quad (11.66)$$

Let:

$$z \triangleq x_{c_4} \quad (11.67)$$

$$\dot{z} \triangleq x_{c_5} = \dot{x}_{c_4} \quad (11.68)$$

Hence:

$$\dot{x}_{c_5} = -25x_{c_5} + 25\Gamma \quad (11.69)$$

$$g = 0.1x_{c_4} + 1.04x_{c_5} - 10x_{c_5} + \frac{651}{R} x_{c_1} - \frac{10}{R} x_{c_2} + \frac{1627.5}{R} x_{c_3} \quad (11.70)$$

Hence, the third term on the r.h.s. of eq. (11.57) can be written as:

$$\delta_{E_c} = 1.9y_2 + 3.1y_3 + 62 \left\{ \frac{651}{R} - \frac{10}{R} \frac{1627.5}{R} 0.1 - 8.96 \right\} \mathbf{x}_c \quad (11.71)$$

$$y_c \triangleq \delta_{E_c} = \left[\frac{40362}{R} \quad - \frac{620}{R} \quad \frac{100905}{R} \quad 6.2 \quad - 555.52 \right] \mathbf{x}_c + [0 \quad 1.9 \quad 3.1] \mathbf{y}$$

Hence:

$$A_c = \begin{bmatrix} 0 & 0 & 0 & 0 & 0 \\ 0 & 0 & 0 & 0 & 0 \\ 0 & 0 & 0 & 0 & 0 \\ 0 & 0 & 0 & 0 & 0 \\ \frac{1627.5}{R} & \frac{-25}{R} & \frac{40687.5}{R} & 0 & -25 \end{bmatrix} \quad (11.72)$$

$$B_c = \begin{bmatrix} 0 & 0 & 1 \\ 65.1 & 0 & 0 \\ 0 & 0 & 0 \\ 0 & 0 & 0 \\ 0 & 0 & 0 \end{bmatrix} \quad (11.73)$$

$$C_c = \left[\frac{40362}{R} \quad \frac{-620}{R} \quad \frac{100905}{R} \quad 6.2 \quad -555.5 \right] \quad (11.74)$$

$$D_c = [0 \ 1.9 \ 3.1] \quad (11.75)$$

$$E = \begin{bmatrix} 0 \\ 0 \\ 1 \\ 0 \\ 0 \end{bmatrix} \quad (11.76)$$

Let:

$$\mathbf{v} = \begin{bmatrix} \mathbf{x} \\ \mathbf{x}_c \end{bmatrix} \quad (11.77)$$

then the closed loop dynamics of the glide-path-coupled control system can be expressed as:

$$\dot{\mathbf{v}} = K\mathbf{v} + L \quad (11.78)$$

where:

$$K = \begin{bmatrix} (A + BD_cC) & BC_c \\ B_cC & A_c \end{bmatrix} \quad (11.79)$$

Table 11.4 Eigenvalues of glide-path system at two values of range

Range = 4 000 m	Range = 200 m
$\lambda_1 = 0.0$	$\lambda_{1,2} = 0.0$
$\lambda_2 = -0.005$	$\lambda_{3,4} = 0.026 \pm j0.024$
$\lambda_3 = -0.013$	$\lambda_5 = -4.004$
$\lambda_4 = -0.12$	$\lambda_6 = -8.91$
$\lambda_{5,6} = -0.186 \pm j0.325$	$\lambda_{7,8} = -1.57 \pm j4.105$
$\lambda_7 = -2.027$	$\lambda_{9,10} = +2.58 \pm j4.77$
$\lambda_{8,9} = -4.21 \pm j6.76$	
$\lambda_{10} = -24.944$	

$$L \triangleq \begin{bmatrix} 0 \\ E \end{bmatrix} \quad (11.80)$$

The eigenvalues of the closed loop system just described, which correspond to values of range, R , of 4 000 m and 200 m, are shown in Table 11.4. It can be deduced from these values of the closed loop roots that at a range of 4 000 m the glide-path-coupled system is stable, but when the range has reduced to 200 m it is unstable. In fact, there is a critical value of range below which the system is unstable.

The treatment above supposes that the glide slope receiver is located at the c.g. of the aircraft, and measures the aircraft's angular deviation from the glide path at the c.g. However, if the aircraft receiver is installed at, say, the nose of the aircraft, the dynamics of the system are affected, as follows. From Figure 11.43, the height measured at the receiver is:

$$h_A \approx h + x_A \theta \quad (11.81)$$

(assuming θ is small). Therefore the flight path angle at the receiver is:

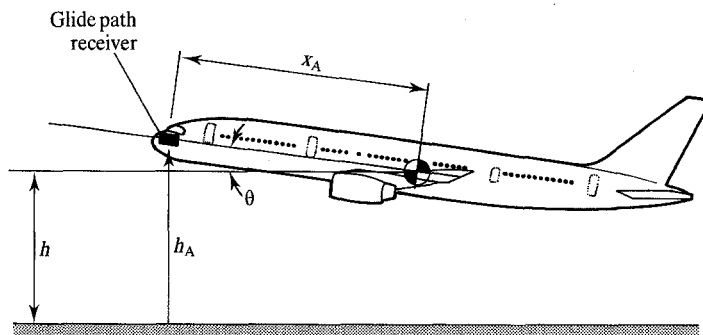


Figure 11.43 Glide path receiver located in aircraft nose.

$$\gamma' = \frac{\dot{h}_A}{U_0} = \frac{\dot{h}}{U_0} + \frac{x_A \dot{\theta}}{U_0} = \gamma + x_A \frac{\dot{\theta}}{U_0} \quad (11.82)$$

$$\therefore \frac{\gamma'(s)}{\theta(s)} = \frac{\gamma(s)}{\theta(s)} + \frac{s x_A}{U_0} \quad (11.83)$$

Thus, the effect of locating the glide path receiver in the aircraft's nose is to introduce a phase advance term into the closed loop dynamics.

11.10 AUTOMATIC LANDING SYSTEM

Although the contribution to the development of airborne automatic landing systems has been international, the basis of most of the operational systems in service is the system developed in the UK by the Blind Landing Experimental Unit (now disbanded) of the Royal Aerospace Establishment. It makes use of the ILS, and the entire automatic landing segment is made up of a number of phases which are shown in Figure 11.44. At the start of the final approach phase (point 1 in Figure 11.44), the aircraft being considered is assumed to be guided on the glide path by a glide-path-coupled control system of the type described in Section 11.9, and to be steered onto the runway centre-line by means of the ILS localizer-coupled control system described in Section 11.8.

What has been described above is a category II automatic landing. What distinguishes landings into the various categories are the conditions of visibility. These categories are summarized in Figure 11.45; it can be seen that each category is defined as a combination of the decision height (DH), i.e. the minimum

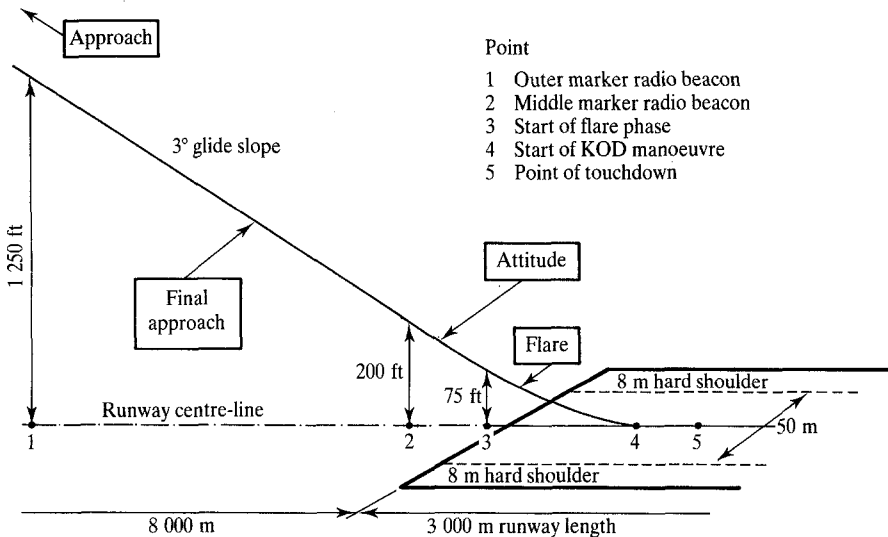


Figure 11.44 BLEU aircraft automatic landing.